Causal Analysis of Graph Signals for Brain Effectome Inference

Srikar Mutnuri, Aniruddha Adiga, Srinivasan Venkatramanan, Madhav V. Marathe
University of Virginia, Charlottesville, VA
{*nmp8rj, aa5dw, sv8nv, mvm7hz*}*@virginia.edu*

***Abstract*—Understanding the directed interactions between brain regions is critical for analyzing neuro-degenerative diseases like Alzheimer's (AD). Traditional functional connectivity (FC) methods capture statistical associations but fail to infer causal relationships, limiting their ability to reveal structural disruptions in disease progression. In this exploratory work, we propose a causal graph inference and spectral analysis framework for EEG signals. Specifically, we leverage Granger causality and spectral graph methods to construct and analyze the effective connectome (effectome) of the brain. Our work reveals that AD networks exhibit lower algebraic connectivity (λ_2), reduced modularity (eigenvalue gaps), and increased structural sensitivity to perturbations, compared to healthy individuals. Additionally, we simulate diffusion processes on the inferred graph topology to model signal propagation, demonstrating disrupted information flow in AD-affected networks.**

I. Introduction

Understanding the neural connection network in the brain (connectome) has been a priority due to the central role it plays in cognitive tasks. While multiple prior works establish a detailed atlas of the human brain, these remain limited to the datasets they work with. Another key issue here is that most studies have worked to establish functional connectivity (FC), which provides inter-regional functional relationships. FC lacks in that it cannot identify asymmetric relationships between these regions, and the resulting network is represented using undirected graphs, with nodes as brain regions and edges between nodes with high functional connectivity. Establishing a cause-effect relationship between the brain regions can be crucial in studying the second order effects of, say, localized degeneration where a disease affects one region of the brain but its effects are seen elsewhere. This can be achieved through effective connectivity (EC) which maps the causal influence of neural activity in a source region on that of a target region. Using (causal) interventions, this can aid the study of the changes in overall behavior when connectivity between two nodes is disrupted (as would be the case in patients with neuro-degenerative diseases which are not constrained by regions). This motivates the key objective behind this project.

A. Research Questions & Approach

We aim to address the following research questions:

- **RQ1**: Can we reliably generate a connectivity model of the brain by applying causal methods on EEG time-series data?
- **RQ2**: Can we use spectral graph analysis to identify the differences in properties of the brain network within healthy individuals and patients with a neuro-degenerative disease (specifically, Alzheimer's Disease)?
- **RQ3**: Can we expand this method to other datasets out-of-the-box?

These questions remain broad, and are intended as a framing device for our work. While the methods are designed to be generalizable, the current work only discusses them in the light of one dataset, thereby constraining the graph size to the number of regions within that data.

Below is the approach taken to achieve the goals stated above (Fig. 1):

- Collect EEG data signals for healthy individuals and patients with Alzheimer's Disease (AD), and preprocess this data to match resolutions and filter higher frequencies
- Perform preliminary analyses on EEG data to study their characteristics
- Use causal modeling to generate an adjacency matrix for brain network - explore the use of Granger Causality to capture complex dynamics
- Perform spectral analysis on the constructed graph using its Laplacian & obtain a Jordan decomposition. Analyze the Fiedler eigenvalue to study the algebraic connectivity of the graph and understand the emergence of communities in the network
- Use a diffusion kernel to simulate stimulus responses in the network

These steps will be elaborated in Appendix B, including a detail on the datasets used.

B. Summary Findings

Some of the key findings are given below:

- While each brain structure is unique, distinguishable features exist in the effectome between healthy individuals and AD patients.
- Eigenvalues (specifically the Fielder value, λ_2) obtained through the spectral analysis show the healthy network being more robust to perturbations (changes in structure), and the AD network sensitive.
- Healthy brain has larger eigengaps (separations between consecutive eigenvalues), which indicates a strong, modular network structure. The AD brain has smaller eigengaps, suggesting reduced connectivity within the network.

An interesting observation was that while our tests to establish **RQ3** required additional pre-processing steps, these were

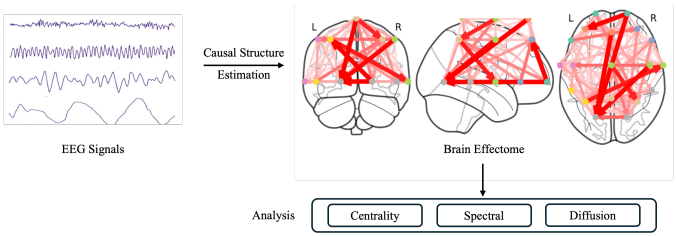

Fig. 1. System Architecture. We estimate the causal structure of the brain from EEG signals, and run spectral analyses to study its properties.

largely due to the data from the sources not being prepared for *causal* analysis. This is further discussed in Appendix B.

II. Data, Experiments & Results

For this work, we consider two datasets - Vicchietti (MV) [1], Miltiadous (AM) [2]. As part of an ongoing effort, we are also experimenting with custom temporal summation of pain dataset (TSP) [3]. Their characteristics are discussed in Appendix B along with a preliminary analysis of the raw data. As mentioned in Section I-A, we present results from tests using the MV dataset. The discussion in the following subsections is the analysis for a randomly picked patient in both the Healthy and AD groups. While the AD effectome generated through the framework is shown in Fig. 1, for completeness all results are presented in the Appendix.

A. Preliminaries

Consider $x_n[t]$, a discrete time series on node v_n in graph $G = (V, E, W)$, where n indexes the nodes of the graph and t the time samples. Let N be the total number of nodes and K be the total number of time samples, and $x[t] \in \mathbb{C}^N$ represents the graph signal at time t. We generate the effectome graph G, with edges E and weights W determined through statistical tests. Within W, w_{ij} represents the weight of the edge between nodes i and j.

B. Network Construction

We construct the effectome weight matrix W through causal inference. This part addresses **RQ1**.

Using Granger causality, we build the effectome, (Fig. 7). At the outset, we see that this is different from the results of Pearson Correlation (correlation $\neq$ causation, Fig. 5 and 6). Additionally, we see a lack of connectivity from the T6 and T5 regions (posterior temporal and parietal occipital junctions) in AD, which signifies impaired memory retrieval and language comprehension. , F8 and Fz have higher connectivity, suggesting possible compensatory mechanism at play. While causation reveals a directional graph, we also symmetrize the matrix to look at both the networks (Fig. 8 and 9). We observe stronger causation in AD brain networks, showing increased and disorganized connectivity, likely due to the pathological processes resulting from the disease. In contrast, the healthy brain network is more uniform. These results are also supported by prior works [4]–[6].

C. Network Analysis

We analyze the properties of the constructed graph G by looking at centrality, spectral decomposition, and study diffusion processes on this graph. This part addresses **RQ2**.

1) Centrality Measures: Fig. 12 shows the centrality measures grouped by the regions described in Appendix B. Typical brain activity happens in the posterior regions, but a higher eigenvector centrality in case of AD patients in the frontal region suggests a compensatory mechanism, likely due to loss of function in the posterior regions [4]–[6].

2) Spectral Analysis - Fiedler Value: An eigendecomposition of the Hermitian Laplacian matrix of G allows us to study its response under variations, especially when perturbed. Fig. 13 shows a plot of eigenvalues, and Fig. 14 shows the graph colored using the Fiedler value λ_2 (FV).

The eigengaps (separations between consecutive eigenvalues) can tell us the robustness of the network. In case of a healthy individual, these are larger, particularly in lower indices, indicating a more well connected and modular network structure. This is also supported by the FV $\lambda_2 \approx 0.5$, indicating a better global connectivity. This means the network can remain well-integrated even if some connections are removed or perturbed. On the other hand, for the AD brain network, the eigenvalues are more closely spaced, suggesting reduced connectivity or weakened modularity in the network. This may reflect the loss of functional integration across brain regions. Similarly, the FV $\lambda_2 \approx 0.3$ indicates a network more sensitive to perturbations.

3) Spectral Analysis - Jordan Decomposition: A Jordan decomposition J of the network can help us understand its sensitivity, and support our findings using λ_2 (Fig. 15). In the healthy network, we see that the diagonals have a smooth gradient, and the super-diagonal is faint or non-existent suggesting minimal coupling between eigenvectors. This indicates a more stable network that is robust to perturbations, and disturbances remain localized. On the other hand, the AD brain network has several sudden changes in the gradient, representing increased dependency or disruption in the system. This indicates a network that is sensitive to perturbations, with disturbances spreading much further within the network.

4) Diffusion Process: To study diffusion over the network, we apply an excitation to nodes Pz, Fp1, and F4 to see how they decay over time. These three nodes are picked at random (Fig. 16). The results remain consistent with the findings above, with the healthy brain network showing a smoother and uniform decay of activations, and the AD brain network having a non-uniform decay.

III. Conclusion & Future Work

This work presented a framework for generating the brain effectome for spectral analysis and explored preliminary findings comparing a healthy brain with one affected by Alzheimer's. Future work will focus on enhancing the model's robustness to input variations (and other datasets) and extending causal methods to account for confounders.

APPENDIX A
RELATED WORKS

The current project covers multiple areas, time series (EEG) signal processing, causal inference, brain connectomes, and network analysis (including spectral graph methods).

Analysis of time-series signals can provide a detailed insight into their nature. Especially, coming to EEG, a key characteristic of this (electro-physiological) data is the presence of periodic (oscillatory) and aperiodic (arrhythmic) activity. While the discussion is out of scope for the current work, some interesting research discussing the emergence of dynamics [7], [8] using these activities exists, and is left for the reader.

Causal inference [9], [10], at a high level, is establishing a cause-effect relationship between different variables through the study of pairwise interactions [11]. Often, we observe the presence of confounders, an external influence driving the relationship. The use of causal methods in understanding the relationship between different neurological processes has been long studied [12], [13], providing us some insights into the inner functioning of the brain.

Much prior work also exists in the study of the brain connectome. Methods like correlation [14], [15], have been widely used, especially in mapping the functional structure and studying its properties, using EEG [16]–[18] and fMRI [19], [20] data. Effective connectome studies rely on causal structure mapping [21], especially by using Granger Causality [22]. Another approach is by looking at the Directed Acyclic Graphs (DAGs) using a graphical criterion known as d-separation, as proposed by Pearl in his seminal work [23].

More recently, scientists at the FlyWire consortium revealed a detailed connectome map of the common fruit fly, capturing the neuronal network of its brain [24], [25]. While they also study some network statistics [26], relevant to the current work is the exploration of how this model gives way to the effectome by [27]. Use of the connectome has also been extended towards studying neuro-degenerative diseases [28], [29]. Spectral graph methods [30], [31] study the properties of the network through the eigendecomposition of its matrices.

These works are largely specific to their domain, and do not tend to work across datasets. The current research aims to generalize the simulation pipeline so as to generate and analyze the brain network.

APPENDIX B
METHODOLOGY

A. Data & Characteristics

Electroencephalography (EEG) remains a key tool in non-invasively capturing brain activity. It is essentially a collection of time-series data, captured using different sensors (nodes) placed at various regions of the brain.

For this project, we look at two datasets - Vicchietti (MV) [1], Miltiadous (AM) [2]. We also consider a custom temporal summation of pain data (TSP) [3] as part of an ongoing effort in future work. The MV and AM datasets contain recordings from both healthy individuals and from patients with Alzheimer's Disease (AD), in resting state (eyes closed). Both follow the the International 10-20 system with 19 electrodes and 2 reference electrodes, as shown in Figure 2. The reference electrodes are only used for establishing the zero voltage and to establish a channel baseline means, and are not considered in the analysis. The pipeline primarily uses the MV dataset, and is evaluated on the AM datasets separately. Some characteristics are given in Table I. Below are the nodes, grouped according to regions.

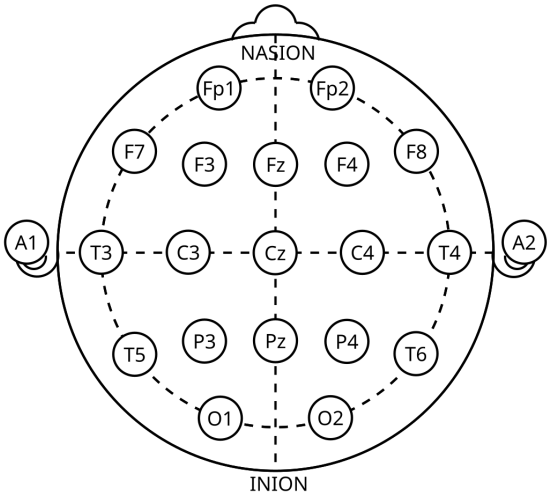

Fig. 2. Electrode placement for the datasets - this is the international 10-20 system with 19 electrodes followed by Vicchietti and Miltiadous

- Frontal: [Fp1, Fp2, F7, F3, Fz, F4, F8]
- Central: [T3, C3, Cz, C4, T4]
- Parietal: [T5, P3, Pz, P4, T6]
- Occipital: [O1, O2]
- 2 reference electrodes: [A1, A2]

While both MV and AM datasets are pre-processed, the data from AM was not processed for causal analysis, and so was not able to capture the causal effects properly. This required framing some causality-preserving pre-processing steps for the raw data using EEGLAB [32]. Normal filters use both forward and backward filtering to nullify the phase delays introduced in the process, but this does not preserve causal relationships. The custom pre-proc step required the use of a forward-only filter which preserves these relationships.

Given that the data is a time-series signal, we can employ multiple ideas from the field of Digital Signal Processing to study its characteristics. More importantly, we are interested in studying the frequency spectra of this data (using Fourier transforms) which shows the components of each frequency within that signal.

Picking on the periodic components, we observe five distinct bands of brain waves - Gamma (over 25-30 Hz), Beta (13-25 Hz), Alpha (8-13 Hz), Theta (4-8 Hz), Delta (0.5-4 Hz), which mark different activities in the brain. It is worth noting that the data from MV lacks the gamma band.

We now use this data to construct the network using statistical methods and causal inference. While this is EEG

TABLE I
COMPARISON OF THE DATASETS.

	Vicchietti (MV)	**Miltiadous (AM)**
Groups	12 Healthy & 80 AD subjects	29 Healthy & 36 AD subjects
Sampling rate	128Hz	500Hz
Data dimensions	(19, 1024)	(19, 299900)
Bands	0.5 – 30 Hz	0.5 – 45 Hz

data, given the nature of our analysis pipeline, we can also use other time-series data such as BOLD (collected from fMRIs) [19]. This testing is out of scope for the current work.

Figure 3 shows a sample of the raw EEG time-series recordings from one patient, with the AD one showing more variance. Using Fourier transform, we look at the frequency spectra in Figure 4. We observe the healthy individuals have more activity in lower frequency bands.

B. Network Construction

While establishing the effectome weight matrix W through causal inference remains the primary objective, we also employ Pearson Correlation to build the functional connectome and validate network connections.

1) Pearson Correlation: The Pearson Correlation (PC) is commonly used to measure the linear correlation between two sets of data, and is a normalized measurement of their covariance, ranging between [-1,1] [33]. When used on brain networks, we obtain functional connectivity. This is described by r:

$$r = \frac{\sum_{i=1}^{n}(x_i - \bar{x})(y_i - \bar{y})}{\sqrt{\sum_{i=1}^{n}(x_i - \bar{x})^2 \sum_{i=1}^{n}(y_i - \bar{y})^2}} \tag{1}$$

where n is the total number of data points for the variables; x_i, and y_i are individual data point from variable X and Y; $\bar{x}$, and $\bar{y}$ their means.

The results are shown in Figure 5 for one patient and 6 across all patients. The graph shows network connectivity between different regions, albeit with varied strengths between the healthy/AD brains. The frontal region shows higher interconnectivity.

2) Causal Inference: While multiple methods exist for Causal inference, a common approach is to use Granger Causality (GC) [34], [35], which simply put, is to check if a variable X *granger causes* another variable Y, by determining if the inclusion of past observations (determined by maximum lag) of the cause reduces the prediction error of the effect using (multi-vector) auto regressive (MVAR) models [36]–[38]. At the most basic version, we pick the elements pairwise, and test the strongest direction of the causal effect [39].

We notate the causation as $X \xrightarrow{G} Y$. The null hypothesis H_0 remains that one variable does not granger cause the other.

To run the tests, we build two models, without and with X_t, the variable X at time t. These are shown by equations 2 and 3.

$$Y_t = \alpha + \sum_{i=1}^{p} \beta_i Y_{t-i} + \epsilon_t \tag{2}$$

$$Y_t = \alpha + \sum_{i=1}^{p} \beta_i Y_{t-i} + \sum_{i=1}^{p} \gamma_i X_{t-i} + \epsilon_t \tag{3}$$

Here, α is the intercept term, β_i & γ_i are the coefficients of the lagged values of Y_t and X_t respectively, and ϵ_t is the error term.

We compare these models using hypothesis tests like F-test or the Wald method and reject outcomes with $p \geq 0.05$. These equations can be extended to include other control variables Z_t, as is typical in real-world networks with multiple influences.

We normalize W to obtain the normalized weight matrix $\tilde{W}$.

$$\tilde{W}_{ij} = \frac{w_{ij}}{\sqrt{d_i^{\text{out}} \cdot d_j^{\text{in}}}} \tag{4}$$

Here, d_i^{in} represents the in-degree and d_i^{out} represents the out-degree of the node. For ease of notation, we will simply notate $\tilde{W}$ as W.

C. Network Analyses

We now run some analyses on G to understand its properties.

1) Centrality Measures: In network analysis, centrality measures are used to identify the most important nodes within a network. Specifically, we look at the degree centrality (number of direct connections a node has), betweenness centrality (number of times a node acts as a bridge along the shortest path between two other nodes), closeness centrality (how close a node is to all other nodes in the network), and eigenvector centrality (a nodes influence based on the influence of its neighbors).

2) Graph Spectral Analysis: We use Graph Signal Processing (GSP) to extend the concepts from signal processing to irregular (graph) domains [40], [41]. The nodes serve as sampling points (notated as $x_n[t]$) and the graph structure provides the connectivity.

More formally, given a graph G with an adjacency matrix A, we can calculate the Graph Laplacian to arrive at the frequency spectrum of the graph.

First, we compute the degree matrix, given by

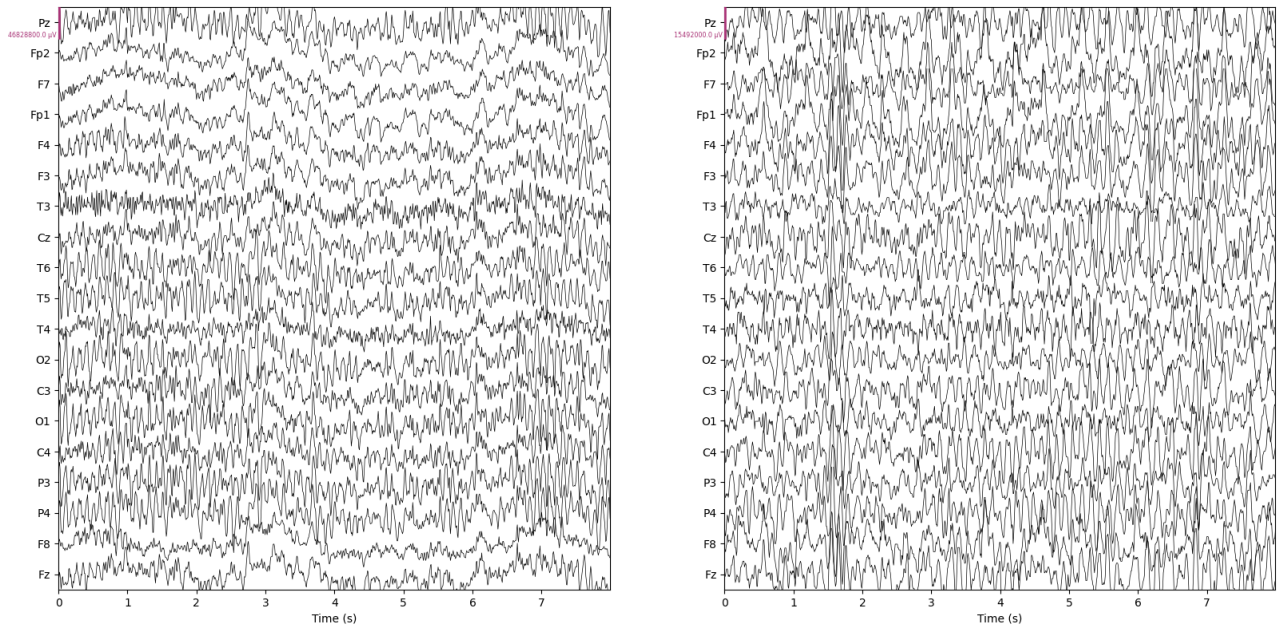

(a) Healthy Individual

(b) AD Patient

Fig. 3. Sample of recorded EEG signals for (a) healthy individual and (b) patient with AD.

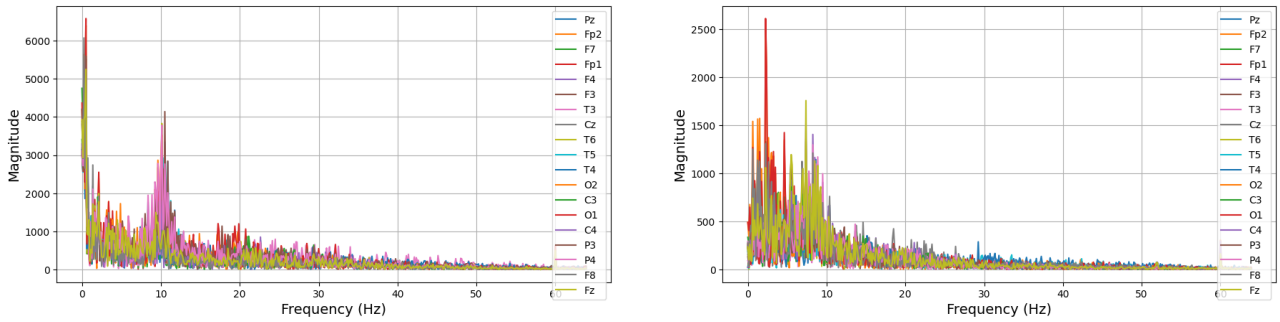

(a) Healthy Individual

(b) AD Patient

Fig. 4. Frequency spectra with the Fourier transform. We can observe the clear differences between the two spectra, with healthy individuals having more activity in the lower frequency bands

$$D_{i,j} = \begin{cases} \sum_{n=1}^{N} W_{i,n}, & \text{if } i = j, \\ 0, & \text{otherwise} \end{cases} \tag{5}$$

This captures the degree of each node of the adjacency matrix. We then calculate the Laplacian as

$$L = D - W \tag{6}$$

We use the Laplacian to build the Graph Fourier Transform through eigendecomposition, and look at the spectral signature for the eigenvalues and eigenvectors:

$$L = \Phi \Delta \Phi^{-1} \tag{7}$$

Where Φ is the eigenvectors matrix, and Δ is the diagonal matrix containing eigenvalues.

A key point of note is that the Laplacian is defined over undirected graphs where the relationship between nodes is symmetric so as to allow for decomposition. To preserve directionality, we use the Hermitian Laplacian L_H [42], which has real eigenvalues and orthogonal eigenvectors.

Fiedler Value: Looking at the eigenvalues obtained from decomposing the Laplacian, the second smallest one λ_2, known as the Fiedler value or the algebraic connectivity of a graph plays a significant role in understanding the connectivity and structure of a graph. It can provide insights into how tightly the graph is connected (higher Fiedler value) and in partitioning the graph.

Jordan Decomposition (JD): The JD provides a representation of a square matrix in terms of its eigenvalues and eigenvectors. For a matrix A, it is expressed as $A = PJP^{-1}$, where P contains the eigenvectors and J is the Jordan matrix.

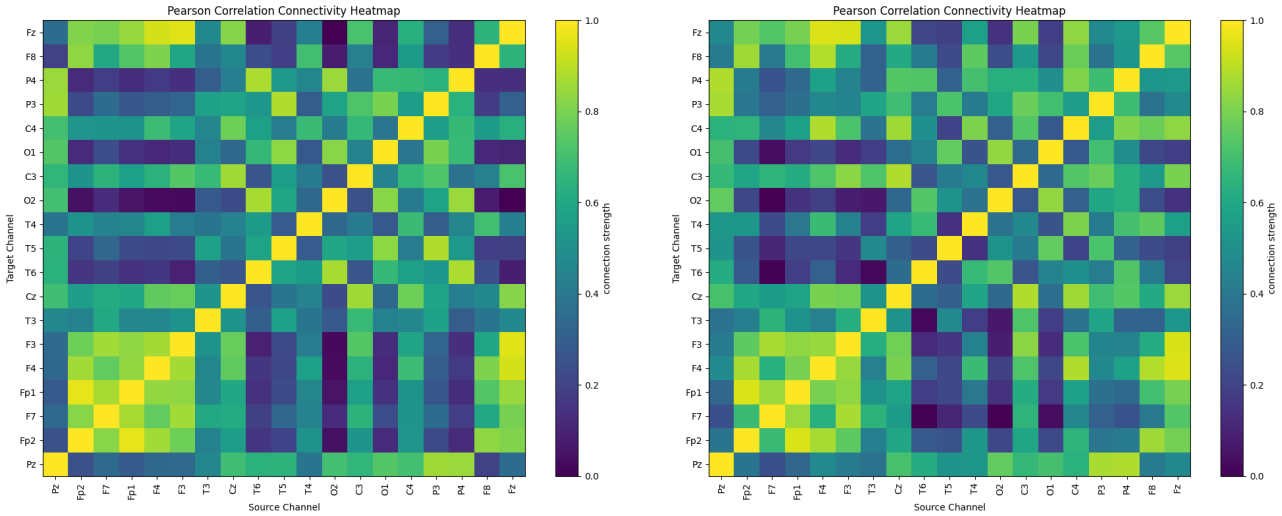

(a) Healthy Individual (b) AD Patient

Fig. 5. Heat map of functional connectome strength, obtained using Pearson Correlation

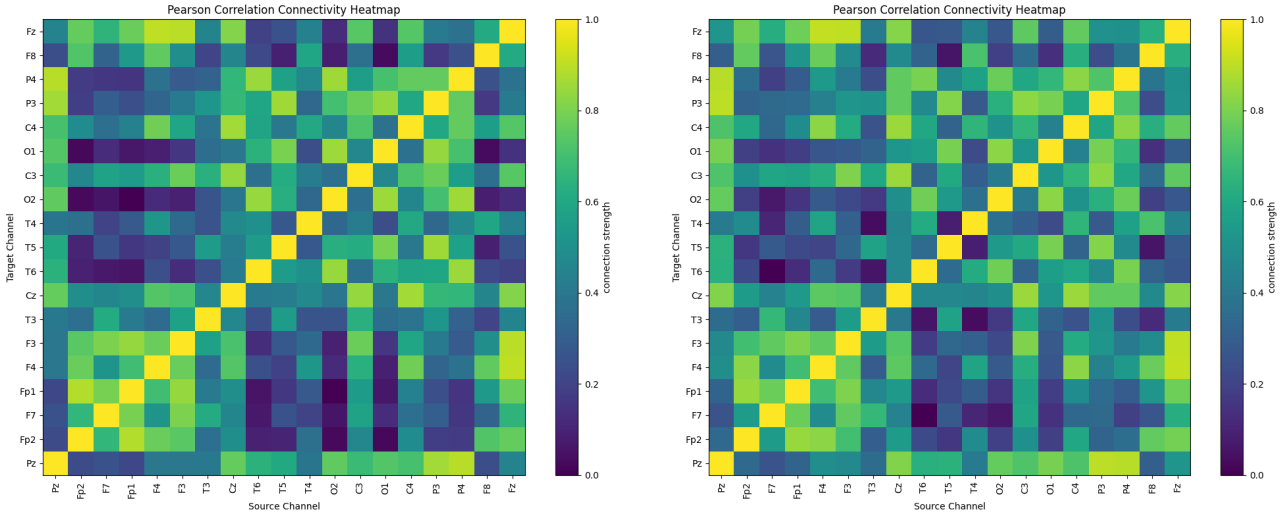

(a) Healthy Individual (b) AD Patient

Fig. 6. Heat map of functional connectome strength across all patients, obtained using Pearson Correlation

J is block diagonal, with each block corresponding to an eigenvalue of A. These Jordan blocks capture the structure of the matrix when A is not diagonalizable.

This is particularly valuable in network analysis for identifying properties like connectivity, robustness and dynamics. Especially looking at eigenvalue gaps, we can understand component connectivity (and community structure) through the Fiedler value. We can also identify similar matrices by reducing the problem of comparing matrices to comparing their Jordan forms. It can also show us how the Laplacian responds to perturbations in the network, which is often observed in neuro-degenerative diseases. Non-diagonalizable Laplacians can indicate the presence of sensitive eigenvalues that are highly affected by small perturbations.

3) Diffusion Processes: In the context of brain networks, Diffusion processes, specifically Reaction-Diffusion processes (RD) provide a powerful framework for modeling the dynamics of neural activity, information transfer, and signal propagation [43], [44]. These processes capture both local interactions between neural populations (reactions) and long-range communication across brain regions (diffusion).

Considering a neural activity or a signal $u_i(t)$, we are interested in studying how it gives rise to local dynamics (reaction) $f(u)$ as it propagates (diffuses) through the graph network G.

This diffusion process is given as:

$$\frac{\partial u}{\partial t} = -DLu \tag{8}$$

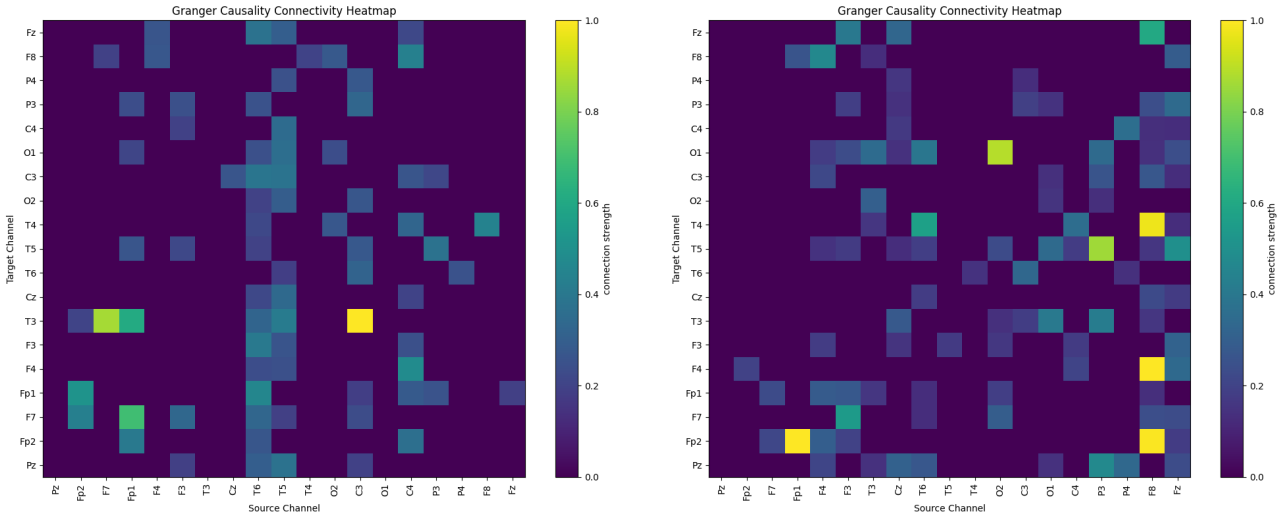

(a) Healthy Individual (b) AD Patient

Fig. 7. Heat map of effective connectome strength, obtained using Granger Causality. We can observe a lack of connectivity from the T6 and T5 regions (posterior temporal and parietal occipital junctions) in AD, which signifies impaired memory retrieval and language comprehension. Interestingly, F8 and Fz have higher connectivity, which shows possible compensatory mechanism at play

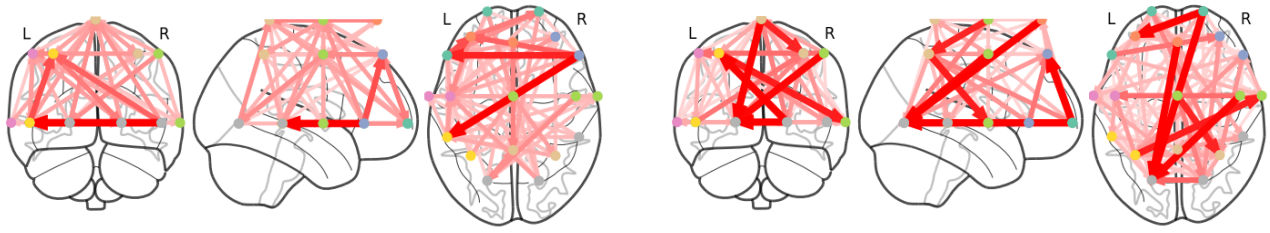

(a) Healthy Individual (b) AD Patient

Fig. 8. Plot of the directed effective connectome, obtained using Granger Causality. Opacity signifies strength of connection, with the most opaque one showing the strongest connection. We observe stronger causation in AD brain networks, showing increased and disorganized connectivity, likely due to the pathological processes resulting from the disease. In contrast, the healthy brain network is more uniform

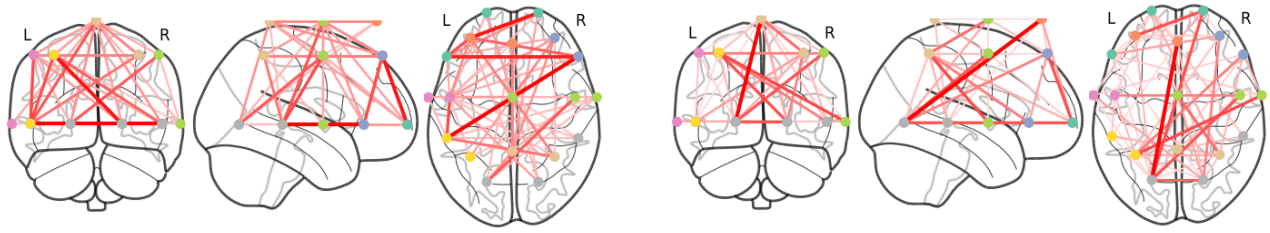

(a) Healthy Individual (b) AD Patient

Fig. 9. Plot of the undirected effective connectome, obtained using Granger Causality. Opacity signifies strength of connection, with the most opaque one showing the strongest connection. The network is symmetrized resulting in an undirected graph. We see similar characteristics as the directed network.

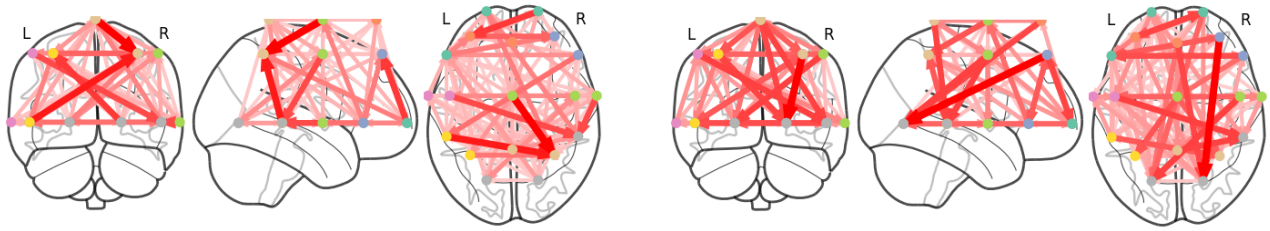

(a) Healthy Individual (b) AD Patient

Fig. 10. Plot of directed effective connectome across all patients, obtained using Granger Causality. As with the single patient result, the AD network show stronger causation compared to the healthy network.

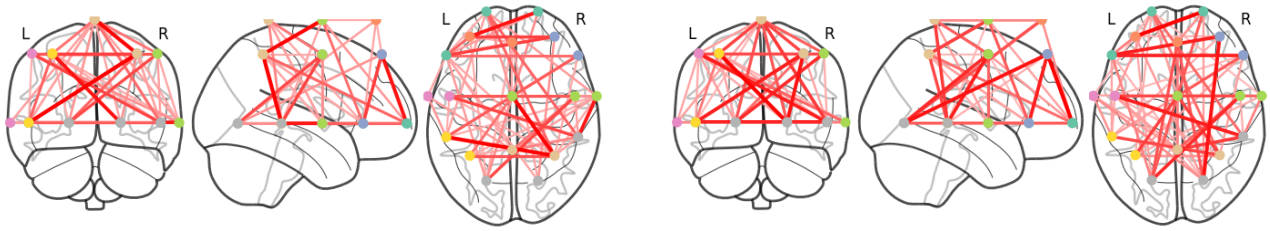

(a) Healthy Individual (b) AD Patient

Fig. 11. Plot of undirected effective connectome across all patients, obtained using Granger Causality. Even with the resulting network being symmetric and undirected, results are similar to the previous figure

The general reaction-diffusion equation for brain networks can be written as:

$$\frac{\partial u}{\partial t} = -DLu + f(u) \tag{9}$$

where $u = [u_1, u_2, \ldots, u_n]^\top$ is the vector of activities at all nodes, L is the graph (hermitian) Laplacian derived from W, and $f(u)$ is the vector of reaction terms.

We can use J obtained earlier for stability analysis [45], but this remains out-of-scope for the current work.

Figures 12, 13, 14, 15, 16 show the results of the pipeline - from network construction through spectral analysis.

D. Tests on other datasets

To test if the network generation works with other datasets out-of-box (as posed in **RQ3**), we run the analysis pipeline on the Miltiadous (AM) dataset.

The AM data was not prepared for *causal* analysis, and as such did not produce viable results out of the box —additional processing steps were needed to ensure that the data is compatible for this purpose. We use a forward-only FIR bandpass filter (0.5 - 45 Hz) that does not correct for phase delays introduced in the process, and run Individual Component Analysis (ICA) decomposition to obtain individual components. As mentioned earlier, we also plan to consider TSP data in this step. It works directly, and we plan to run extensive analysis on this data as part of future work. As an initial observation, this data is more granular, and reveals better causal mapping at a lower level compared to the MV dataset.

REFERENCES

[1] M. L. Vicchietti, F. M. Ramos, L. E. Betting, and A. S. Campanharo, "Computational methods of eeg signals analysis for alzheimer's disease classification," *Scientific Reports*, vol. 13, no. 1, p. 8184, 2023.

[2] A. Miltiadous, K. D. Tzimourta, T. Afrantou, P. Ioannidis, N. Grigoriadis, D. G. Tsalikakis, P. Angelidis, M. G. Tsipouras, E. Glavas, N. Giannakeas *et al.*, "A dataset of scalp eeg recordings of alzheimer's disease, frontotemporal dementia and healthy subjects from routine eeg," *Data*, vol. 8, no. 6, p. 95, 2023.

[3] D. Wang, S. Ye, X. Zhang, W. Carter, P. Finan, M. Quigg, S. Moosa, W. J. Elias, and C.-C. Liu, "Temporal summation of pain varies across body region: A cutaneous laser stimulation study," *Journal of Pain*, 2024, under revision.

[4] M. M. Engels, C. J. Stam, W. M. van der Flier, P. Scheltens, H. de Waal, and E. C. van Straaten, "Declining functional connectivity and changing hub locations in alzheimer's disease: an eeg study," *BMC neurology*, vol. 15, pp. 1–8, 2015.

[5] M. A. Binnewijzend, S. M. Adriaanse, W. M. Van der Flier, C. E. Teunissen, J. C. De Munck, C. J. Stam, P. Scheltens, B. N. Van Berckel, F. Barkhof, and A. M. Wink, "Brain network alterations in alzheimer's disease measured by eigenvector centrality in fmri are related to cognition and csf biomarkers," *Human brain mapping*, vol. 35, no. 5, pp. 2383–2393, 2014.

[6] E. J. Sanz-Arigita, M. M. Schoonheim, J. S. Damoiseaux, S. A. Rombouts, E. Maris, F. Barkhof, P. Scheltens, and C. J. Stam, "Loss of 'small-world'networks in alzheimer's disease: graph analysis of fmri resting-state functional connectivity," *PloS one*, vol. 5, no. 11, p. e13788, 2010.

[7] P. Pourdavood and M. Jacob, "Eeg spectral attractors identify a geometric core of brain dynamics," *Patterns*, vol. 5, no. 9, 2024.

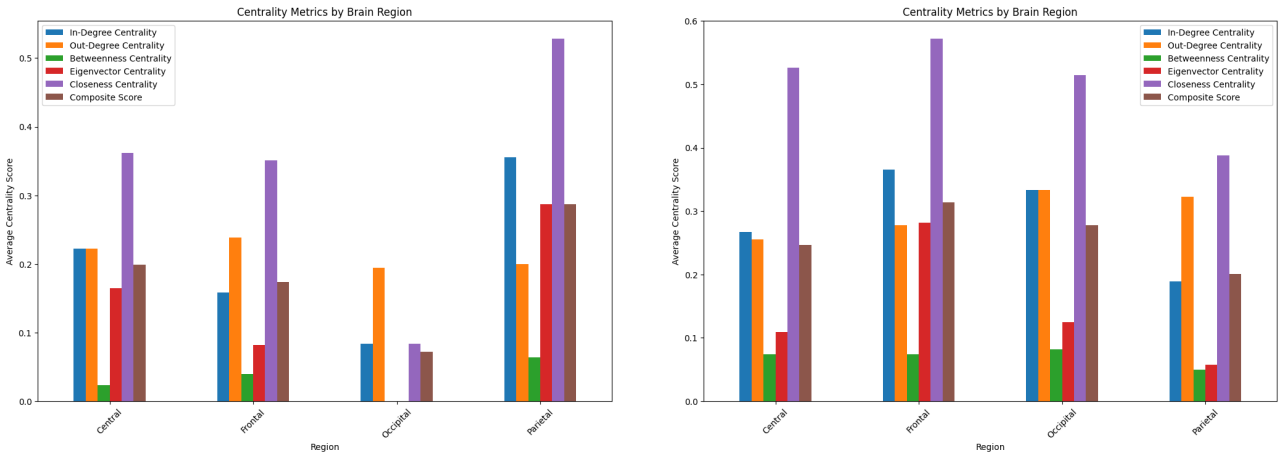

(a) Healthy Individual (b) AD Patient

Fig. 12. Centrality measures grouped by regions. Typical brain activity happens in the posterior regions, but a higher eigenvector centrality in case of AD patients in the frontal region shows a compensatory mechanism at play, likely due to loss of function in the posterior regions

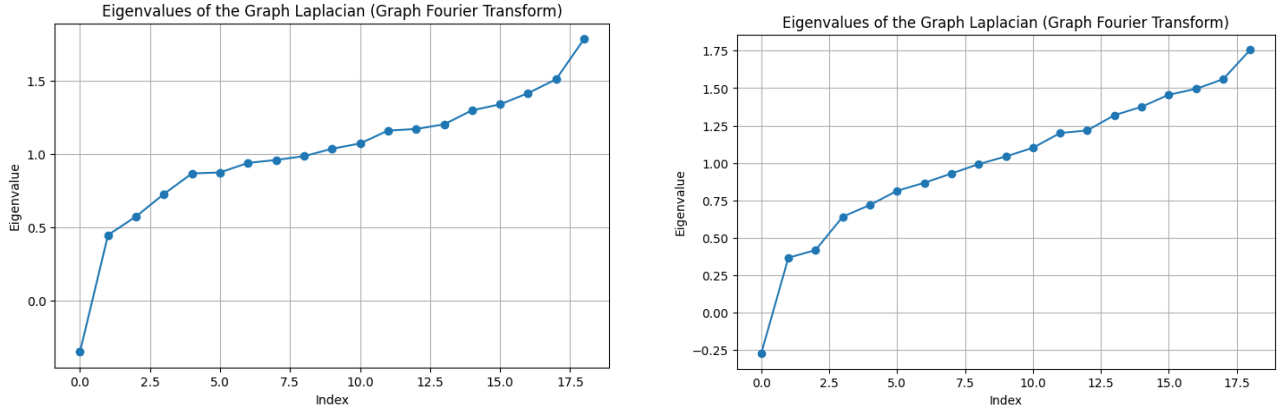

(a) Healthy Individual (b) AD Patient

Fig. 13. Eigenvalues obtained by decomposing the Hermitian Laplacian of the connectome. The eigenvalues of the healthy individual's graph show larger separations between consecutive values, particularly at lower indices, indicating a more well-connected and modular network structure, as larger eigenvalue gaps are often associated with robust connectivity and distinct communities. For the AD patient, the eigenvalues are more closely spaced, suggesting reduced connectivity or weakened modularity in the network. This may reflect the loss of functional integration across brain regions.

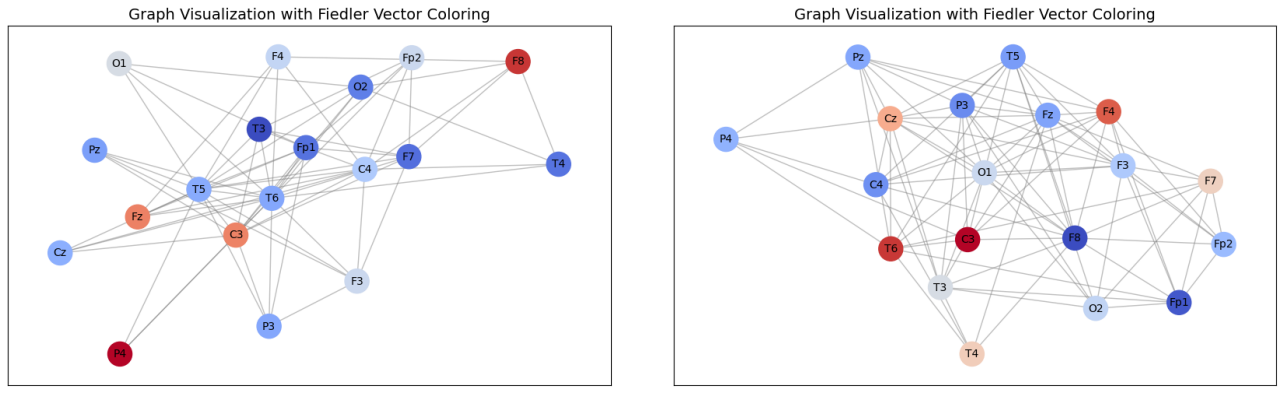

(a) Healthy Individual (b) AD Patient

Fig. 14. Graph coloring using the Fiedler value. From our analysis, we can see that the healthy network has a larger value (around 0.5, indicating a better global connectivity, which means the network can remain well-integrated even if some connections are removed or perturbed. The value of AD network is smaller (around 0.3, which indicate a network more sensitive to perturbations.

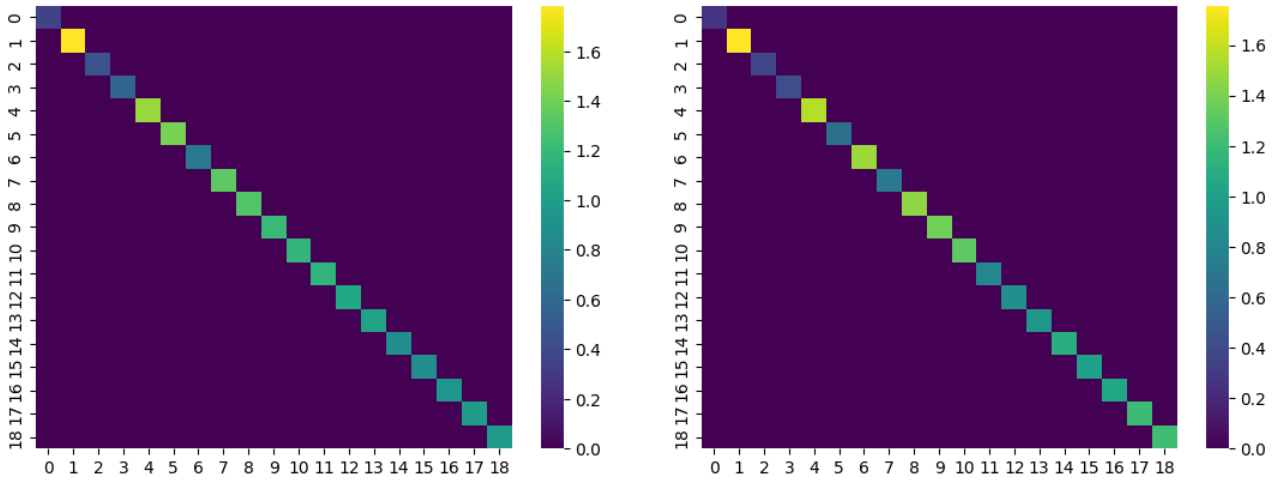

(a) Healthy Individual (b) AD Patient

Fig. 15. Heat map of the Jordan decomposition J. We plot $Re(J)$. We notice a smoother gradient in healthy network, compared to the AD network.

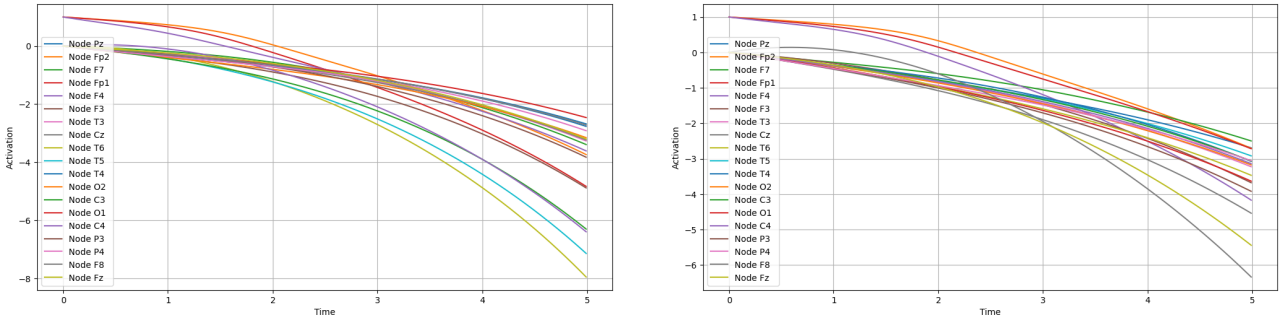

(a) Healthy Individual (b) AD Patient

Fig. 16. Diffusion process over the graph G showing the decay of activations to nodes Pz, Fp1, and F4. Healthy network has a more uniform decay, while AD is non-uniform.

[8] D. Benozzo, G. Baron, L. Coletta, A. Chiuso, A. Gozzi, and A. Bertoldo, "Macroscale coupling between structural and effective connectivity in the mouse brain," *Scientific Reports*, vol. 14, no. 1, p. 3142, 2024.

[9] J. Pearl, "Causal inference," *Causality: objectives and assessment*, pp. 39–58, 2010.

[10] V. J. López-Madrona, F. S. Matias, C. R. Mirasso, S. Canals, and E. Pereda, "Inferring correlations associated to causal interactions in brain signals using autoregressive models," *Scientific reports*, vol. 9, no. 1, p. 17041, 2019.

[11] R. E. Rosch, D. R. Burrows, C. W. Lynn, and A. Ashourvan, "Spontaneous brain activity emerges from pairwise interactions in the larval zebrafish brain," *Physical Review X*, vol. 14, no. 3, p. 031050, 2024.

[12] C. Kayser and L. Shams, "Multisensory causal inference in the brain," *PLoS biology*, vol. 13, no. 2, p. e1002075, 2015.

[13] S. H. Siddiqi, K. P. Kording, J. Parvizi, and M. D. Fox, "Causal mapping of human brain function," *Nature reviews neuroscience*, vol. 23, no. 6, pp. 361–375, 2022.

[14] N. Masuda, Z. M. Boyd, D. Garlaschelli, and P. J. Mucha, "Correlation networks: Interdisciplinary approaches beyond thresholding," *arXiv preprint arXiv:2311.09536*, 2023.

[15] L. Astolfi, F. Cincotti, D. Mattia, F. D. V. Fallani, A. Tocci, A. Colosimo, S. Salinari, M. G. Marciani, W. Hesse, H. Witte *et al.*, "Tracking the time-varying cortical connectivity patterns by adaptive multivariate estimators," *IEEE Transactions on Biomedical Engineering*, vol. 55, no. 3, pp. 902–913, 2008.

[16] G. Chiarion, L. Sparacino, Y. Antonacci, L. Faes, and L. Mesin, "Connectivity analysis in eeg data: a tutorial review of the state of the art and emerging trends," *Bioengineering*, vol. 10, no. 3, p. 372, 2023.

[17] S. Kulkarni and D. S. Bassett, "Towards principles of brain network organization and function," *arXiv preprint arXiv:2408.02640*, 2024.

[18] L. Päeske, T. Uudeberg, H. Hinrikus, J. Lass, and M. Bachmann, "Correlation between electroencephalographic markers in the healthy brain," *Scientific Reports*, vol. 13, no. 1, p. 6307, 2023.

[19] S. Ogawa, T.-M. Lee, A. R. Kay, and D. W. Tank, "Brain magnetic resonance imaging with contrast dependent on blood oxygenation." *proceedings of the National Academy of Sciences*, vol. 87, no. 24, pp. 9868–9872, 1990.

[20] R. D. Mill, J. L. Hamilton, E. C. Winfield, N. Lalta, R. H. Chen, and M. W. Cole, "Network modeling of dynamic brain interactions predicts emergence of neural information that supports human cognitive behavior," *PLoS biology*, vol. 20, no. 8, p. e3001686, 2022.

[21] D. Chicharro and S. Panzeri, "Algorithms of causal inference for the analysis of effective connectivity among brain regions," *Frontiers in neuroinformatics*, vol. 8, p. 64, 2014.

[22] U. Brainstorm Team, "Granger causality," 2024, accessed: 2024-12-01.

[23] J. Pearl, "Fusion, propagation, and structuring in belief networks," in *Probabilistic and Causal Inference: The Works of Judea Pearl*, 2022, pp. 139–188.

[24] S. Dorkenwald, A. Matsliah, A. R. Sterling, P. Schlegel, S.-C. Yu, C. E. McKellar, A. Lin, M. Costa, K. Eichler, Y. Yin *et al.*, "Neuronal wiring diagram of an adult brain," *Nature*, vol. 634, no. 8032, pp. 124–138, 2024.

[25] P. Schlegel, Y. Yin, A. S. Bates, S. Dorkenwald, K. Eichler, P. Brooks, D. S. Han, M. Gkantia, M. Dos Santos, E. J. Munnelly *et al.*, "Whole-brain annotation and multi-connectome cell typing of drosophila," *Nature*, vol. 634, no. 8032, pp. 139–152, 2024.

[26] A. Lin, R. Yang, S. Dorkenwald, A. Matsliah, A. R. Sterling, P. Schlegel, S.-c. Yu, C. E. McKellar, M. Costa, K. Eichler *et al.*, "Network statistics of the whole-brain connectome of drosophila," *Nature*, vol. 634, no. 8032, pp. 153–165, 2024.

[27] D. A. Pospisil, M. J. Aragon, S. Dorkenwald, A. Matsliah, A. R. Sterling, P. Schlegel, S.-c. Yu, C. E. McKellar, M. Costa, K. Eichler *et al.*, "The fly connectome reveals a path to the effectome," *Nature*, vol. 634, no. 8032, pp. 201–209, 2024.

[28] A. Kabbara, W. El Falou, M. Khalil, F. Wendling, and M. Hassan, "The dynamic functional core network of the human brain at rest," *Scientific reports*, vol. 7, no. 1, p. 2936, 2017.

[29] A. Kabbara, G. Robert, M. Khalil, M. Verin, P. Benquet, and M. Hassan, "An electroencephalography connectome predictive model of major depressive disorder severity," *Scientific Reports*, vol. 12, no. 1, p. 6816, 2022.

[30] K. Glomb, J. R. Queralt, D. Pascucci, M. Defferrard, S. Tourbier, M. Carboni, M. Rubega, S. Vulliemoz, G. Plomp, and P. Hagmann, "Connectome spectral analysis to track eeg task dynamics on a subsecond scale," *NeuroImage*, vol. 221, p. 117137, 2020.

[31] E. Bullmore and O. Sporns, "Complex brain networks: graph theoretical analysis of structural and functional systems," *Nature reviews neuroscience*, vol. 10, no. 3, pp. 186–198, 2009.

[32] A. Delorme and S. Makeig, "Eeglab: an open source toolbox for analysis of single-trial eeg dynamics including independent component analysis," *Journal of neuroscience methods*, vol. 134, no. 1, pp. 9–21, 2004.

[33] K. Pearson, "Vii. note on regression and inheritance in the case of two parents," *proceedings of the royal society of London*, vol. 58, no. 347-352, pp. 240–242, 1895.

[34] C. Granger, "Investigating causal relations by econometric models and cross-spectral methods," in *Essays in econometrics: collected papers of Clive WJ Granger*, 2001, pp. 31–47.

[35] W. D. Penny, "Comparing dynamic causal models using aic, bic and free energy," *Neuroimage*, vol. 59, no. 1, pp. 319–330, 2012.

[36] A. K. Seth, "A matlab toolbox for granger causal connectivity analysis," *Journal of neuroscience methods*, vol. 186, no. 2, pp. 262–273, 2010.

[37] J. Cui, L. Xu, S. L. Bressler, M. Ding, and H. Liang, "Bsmart: a matlab/c toolbox for analysis of multichannel neural time series," *Neural Networks*, vol. 21, no. 8, pp. 1094–1104, 2008.

[38] Y. Chen, S. L. Bressler, and M. Ding, "Frequency decomposition of conditional granger causality and application to multivariate neural field potential data," *Journal of neuroscience methods*, vol. 150, no. 2, pp. 228–237, 2006.

[39] L. Barnett and A. K. Seth, "Behaviour of granger causality under filtering: theoretical invariance and practical application," *Journal of neuroscience methods*, vol. 201, no. 2, pp. 404–419, 2011.

[40] A. Ortega, P. Frossard, J. Kovačević, J. M. Moura, and P. Vandergheynst, "Graph signal processing: Overview, challenges, and applications," *Proceedings of the IEEE*, vol. 106, no. 5, pp. 808–828, 2018.

[41] D. I. Shuman, S. K. Narang, P. Frossard, A. Ortega, and P. Vandergheynst, "The emerging field of signal processing on graphs: Extending high-dimensional data analysis to networks and other irregular domains," *IEEE signal processing magazine*, vol. 30, no. 3, pp. 83–98, 2013.

[42] S. Furutani, T. Shibahara, M. Akiyama, K. Hato, and M. Aida, "Graph signal processing for directed graphs based on the hermitian laplacian," in *Machine Learning and Knowledge Discovery in Databases: European Conference, ECML PKDD 2019, Würzburg, Germany, September 16–20, 2019, Proceedings, Part I*. Springer, 2020, pp. 447–463.

[43] O. Schmitt, C. Nitzsche, P. Eipert, V. Prathapan, M.-T. Hütt, and C. C. Hilgetag, "Reaction-diffusion models in weighted and directed connectomes," *PLOS Computational Biology*, vol. 18, no. 10, p. e1010507, 2022.

[44] J. Zhang, D. Yang, W. He, G. Wu, and M. Chen, "A network-guided reaction-diffusion model of at [n] biomarkers in alzheimer's disease," in *2020 IEEE 20th International Conference on Bioinformatics and Bioengineering (BIBE)*. IEEE, 2020, pp. 222–229.

[45] C. Rao, P. Ren, Q. Wang, O. Buyukozturk, H. Sun, and Y. Liu, "Encoding physics to learn reaction–diffusion processes," *Nature Machine Intelligence*, vol. 5, no. 7, pp. 765–779, 2023.